Planta (2002) 216: 72–82
DOI 10.1007/s00425-002-0884-4

ORIGINAL ARTICLE

A.L. Samuels · K.H. Rensing · C.J. Douglas
S.D. Mansfield · D.P. Dharmawardhana · B.E. Ellis

Cellular machinery of wood production: differentiation of secondary xylem in *Pinus contorta* var. *latifolia*

Received: 8 April 2002 / Accepted: 29 July 2002

Abstract The objectives of this study were to define cell structure during pine secondary xylem development and to integrate this information with current knowledge of the biochemistry and physiology of secondary cell wall biosynthesis in gymnosperms. Lodgepole pine (*Pinus contorta* var. *latifolia* Englem.) cambium and secondary xylem were cryofixed using high pressure freezing and freeze-substitution which allowed excellent preservation of the cell structure of developing secondary xylem and enabled high-resolution transmission electron microscopic viewing of these cells for the first time. In contrast to their precursors in the adjacent cambial zone, developing tracheids were active in secondary wall deposition, with abundant cortical microtubules and developing bordered pits. These cells were also characterized by unusual Golgi structures: the *trans*-Golgi network was highly developed and the associated vesicles were large and darkly stained. These unusual Golgi structures persisted throughout the period of xylem maturation until programmed cell death occurred. Immuno-cytochemistry and enzyme-gold probes were used to investigate the distribution of key secretory products (mannans) and a lignification-associated enzyme (coniferin β-glucosidase) during xylogenesis. Mannans were localized to the secondary cell wall, the *trans*-Golgi cisternae and *trans*-Golgi network vesicles of developing xylem. Coniferin β-glucosidase was found only in the secondary cell wall. The cell wall localization of coniferin β-glucosidase, the enzyme responsible for cleaving glucose from coniferin to generate free coniferyl alcohol, provides a mechanism to de-glucosylate monolignols *in muro*. A two-step model of lignification of conifer tracheids is proposed. First, Golgi-mediated secretion deposits monolignols into the cell wall, where they polymerize in cell corners and middle lamella. Secondly, cell lysis releases stored, vacuolar monolignol glucosides into the wall where they are deglucosylated and their polymerization is influenced by the wall environment including the lignin deposited earlier.

Keywords Lignification · Mannan · *Pinus* · Secondary cell wall · Tracheid · Xylogenesis

Abbreviations BSA: bovine serum albumin · CβG: coniferin beta-glucosidase · TGN: *trans*-Golgi network

Introduction

Given the ecological and economic significance of trees, the development of the secondary vascular system is an important and fascinating biological process (Chaffey 1999). Conifers provide an excellent experimental system for studying wood formation because the secondary xylem consists of a relatively homogenous cell population of long tubular tracheids (Esau 1965). During secondary xylem differentiation, thin-walled precursor cambial cells undergo dramatic transformations including secondary cell wall deposition, bordered pit formation, lignification and programmed cell death (Savidge 1996).

To fully understand these developmental milestones, a detailed knowledge of the cell structure of developing tracheids is necessary. However, the cell structure of

Dedicated to Nikolaus Amrhein, Zürich, on the occasion of his 60th birthday.

A.L. Samuels (✉) · K.H. Rensing · C.J. Douglas
Department of Botany,
University of British Columbia,
Vancouver, BC, Canada, V6T 1Z4
E-mail: lsamuels@interchange.ubc.ca
Tel.: +1-604-8225469
Fax: +1-604-8226089

D.P. Dharmawardhana · B.E. Ellis
Biotechnology Laboratory,
University of British Columbia,
Vancouver, BC, Canada, V6T 1Z3

S.D. Mansfield
Department of Wood Sciences,
University of British Columbia,
Vancouver, BC, Canada, V6T 1Z4

differentiating secondary xylem has been difficult, if not impossible, to preserve for electron microscopy using conventional chemical fixatives. Earlier studies, which used chemical fixatives to preserve cells for electron microscopy, were unable to describe intact cell structure due to the slow and disruptive action of chemical fixatives on cell structure (Srivastava and O'Brien 1966; Murmanis and Sachs 1969; Barnett 1977). This is especially apparent in the late stages of development when hydrolytic enzymes accumulated in the vacuole are released as the cells are immersed in conventional chemical fixatives. The cell structure of the developing xylem observed following chemical fixation included the "fragmentary nature of the plasmalemma" and "dismembered" Golgi apparatus (Cronshaw and Wardrop 1964). These studies did not provide accurate information on the endomembranes of the developing xylem cells.

The developing xylem of conifers is highly specialized for secondary cell wall production with a biochemical commitment to lignification (Savidge 1989). During secondary wall formation, a complex architecture of polysaccharides is first established and the resulting structure is then impregnated with lignin (reviewed by Donaldson 2001). The thin, expansible primary cell wall of cambium cells contains relatively more xyloglucans and pectins and less cellulose than does the secondary wall, which consists of extensive cellulose deposition embedded in galactoglucomannan. The change in the nature of the primary and secondary cell wall has been described for the wall itself (Terashima et al. 1998), but the role of the endomembrane system of the cell in producing the hemicelluloses of the secondary cell wall has not been well characterized. To follow mannan biosynthesis in the *Pinus contorta* secondary vascular system, we used an enzyme-gold cytochemical probe which was specific for mannans.

The cambial sap of conifers contains high levels of coniferin, the glucoside of the monolignol coniferyl alcohol (Freudenberg and Harkin 1963; Terazawa et al. 1984). In protoplasts, coniferin has been estimated to reach a concentration of 1 mM on a fresh weight basis (Leinhos and Savidge 1994). This lignin precursor must be de-glucosylated to coniferyl alcohol by a coniferin-specific β-glucosidase before dehydrogenative polymerization of lignin can proceed. A candidate *Pinus contorta* coniferin-specific β-glucosidase has been characterized at the molecular and biochemical levels (Dharmawardhana et al. 1995, 1999). The specificity of this glucosidase towards coniferin, and the localization of coniferin specific β-glucosidase enzyme activity and coniferin specific β-glucosidase mRNA to developing xylem, support a role for this enzyme in the lignification process (Whetton and Sederoff 1995). Identification of the subcellular location of the coniferin β-glucosidase would help determine whether lignin precursors are exported as glucosides or as aglycones, an important distinction for predicting the gene products and mechanisms involved in monolignol export and incorporation into lignin.

The goals of this study were to define important cell structures involved in conifer xylogenesis and to relate this structural information to the mechanism of secondary cell wall synthesis, including hemicellulose deposition and guaiacyl lignin formation. To avoid problems with chemical fixation of developing xylem, lodgepole pine (*P. contorta* var. *latifolia* Englem.) cambium and associated secondary xylem were cryofixed using high pressure freezing and freeze-substitution. This rapid freezing technique stabilized the cell structure and allowed an unprecedented high resolution examination of these cells, particularly of the endomembrane system, by transmission electron microscopy. The results provide a baseline of cell structure information to allow model building and integration of the biochemistry of guaiacyl lignin deposition with the cell biology of xylogenesis.

Materials and methods

High pressure freezing/freeze substitution

Inner bark of *Pinus contorta* var. *latifolia* was collected from 2-year-old seedlings grown in growth chambers for 2–4 weeks following dormancy in cold storage (4°C, dark), or from field sites in Boulder County, Colorado, USA in June of 1998 and 1999. Cambium, developing and mature xylem were dissected with double edged razor blades and immersed in 0.2 M sucrose as an extracellular cryoprotectant. Sucrose concentrations up to 0.4 M did not cause plasmolysis or alter cytoplasmic streaming in conifer cambial cells over a 4-h period of observations (Rensing 2002). Slices of cambium and associated developing xylem (0.4 mm × 0.2 mm) were frozen with a Baltec High Pressure Freezer in two 'B' hats (Ted Pella, Redding, Calif., USA) to make the largest chamber possible. The hats were immediately transferred to cryovials containing freeze substitution medium consisting of 2% osmium tetroxide in acetone with 8% dimethoxypropane. Freeze substitution was carried out for 4–5 days at –80°C by incubating the cryovials in an acetone/dry ice slush, followed by transfer of the cryovials into a metal block precooled to –20 C for 2 h. The metal block was then moved to 4°C for 2 h, then 20°C for 2 h to allow reaction of fixatives. The samples were rinsed several times in anhydrous acetone and the sample holders removed from the cryovials. The early stages of embedding were found to be critical to the success of resin infiltration through the sample. One drop of Spurr's or JBEMBED epoxy resins was added every 5–10 min to 1 ml of acetone containing the samples until the concentration of resin was approximately 10% (v/v), at which point the samples were left overnight on a rotator. The concentration of resin was then increased, every 4 h, in steps to 25%, 50%, and then 75%, overnight. After a full day in 100% resin, the samples were polymerized overnight at 60°C. For immuno-gold work, samples were substituted in 0.25% glutaraldehyde in acetone, followed by embedding in LRWhite resin which was infiltrated as above and polymerized at 60°C in sealed flat-bottomed BEEM capsules (to exclude air/oxygen). An alternative method was substitution in acetone/8%DMP at –80°C for 4–5 days by incubating the cryovials in an acetone/dry ice slush, followed by transfer of the cryovials into a metal block precooled to –20°C. LRGold resin was infiltrated into the samples for 24 h in steps of 25%, 50%, 75%, and 100% at –20°C and polymerized at –20°C using ultraviolet light. Even with the extended infiltration time, samples prepared using this protocol often had separation of cells in the cambium in the middle lamella and variations in section thickness and quality. The room temperature embedding using LRWhite was superior for morphology but did not seem to preserve antigenicity as well.

These small flaws are typical of the compromises in morphological quality that are made for optimal preservation of antigenicity when preparing samples for immunolabelling.

Light microscope sections were examined for intact cells, as the initial dissection of the pine cambium resulted in loss of cell contents in 40–60% of the cells examined. Samples that contained intact developing xylem cells were thin sectioned using a Reichert Ultracut E and sections mounted on 200 mesh formvar coated copper grids. Following post-staining in 2% aqueous uranyl acetate (30 min) and Reynold's lead citrate (5 min), samples were viewed with a Zeiss EM10. Alkaline bismuth treatment of sections, which stains periodate-reactive 1,2-glycols such as polysaccharides, has previously been shown to strongly label plant Golgi vesicles (Park et al. 1987) and was performed as described in Shinji et al. (1976).

Lignin histochemistry

The secondary vascular cambium and associated tissues embedded in LRWhite were cut into 0.5-μm sections using a Reichert OMU3 microtome and stained for 30 s with 1% toluidine blue in 1% sodium borate. Lignified cell walls appeared turquoise coloured while non-lignified walls were purple. For the Mäule reaction, 0.5-μm sections of LRWhite-embedded samples were treated with 1% potassium permanganate for 5–10 min, washed in distilled water, and mounted in ammonium hydroxide. Lignified cell walls appeared purple-brown. For phloroglucinol staining, LRWhite sections were treated with 1% phloroglucinol in 95% ethanol for 1–2 min followed by treatment with a few drops of concentrated HCl and were examined in the acid medium. Lignified cell walls appeared reddish-pink. For autofluorescence, unstained 0.5-μm sections of samples embedded in LRWhite were examined with a Zeiss Axiophot epifluorescence microscope using a Zeiss filter 18 (excitation at BP390–440 nm and emission at 470 nm). The number of cells between the most mature cambium cell and the cell showing the first signs of lignification was counted for each histochemical test. Live protoplasts in the developing xylem were counted on 0.5-μm sections stained with toluidine blue, but as the cell contents may be lost during dissection from the tree seedling, these numbers represent only a rough estimate.

Immunogold and enzyme/gold labelling

Mannanase-gold was prepared by the conjugation of colloidal gold particles and purified *Aspergillus* sp. mannanase. A glucomannan-specific mannanase was purified to homogeneity, based on SDS PAGE electrophoresis, from a commercially available crude acidic hemicellulase (Gammanase, Novozymes) derived from *Aspergillus* sp. Briefly, a three-step chromatographic purification protocol was employed. Initially, proteins in the crude enzyme preparation were separated by ion exchange chromatography using a DEAE Sephadex packed column. The proteins were eluted using a linear gradient of 20 mM Tris-HCl to 20 mM Tris-HCl + 0.6 M NaCl (pH 6.8), at a flow rate of 1 ml/min. The fractions containing mannanase activity were pooled and concentrated using an Amicon ultrafiltration unit equipped with a Diaflo YM10 membrane with a 10 kDa cutoff. The concentrated fraction was then subjected to hydrophobic interaction chromatography on a Phenyl Sepharose CL-4B-packed column using a linear gradient of 500 mM to 10 mM ammonium sulphate (pH 4.3) at a flow rate of 1 ml/min. The fractions specific for glucomannan were again collected, pooled and concentrated by ultrafiltration. The concentrated sample was then purified to homogeneity by gel filtration chromatography on a Superose 12 HR10/30 column (Amersham Pharmacia Biotech) using 50 mM sodium acetate (pH 4.5) buffer at a flow rate of 1 ml/min. Mannanase activity was determined and monitored on 1% (w/v) Konjac glucomannan in sodium acetate buffer (pH 4.5). Reducing sugars generated from the cleavage of glycosyl linkages in the substrate were quantified by reaction with dinitrosalicylic acid and measured spectrophotometrically at 540 nm, as described previously (Wood and Bhat 1988; Gübitz et al. 1996).

Purified mannanase or bovine serum albumin (BSA, as a control) were conjugated to colloidal gold particles (Samuels et al. 1995). Gold particles of 15 nm diameter were prepared by reduction of tetrachloroauric acid by sodium citrate. Five millilitres of 0.2% tetrachloroauric acid were added to 95 ml distilled deionized water and boiled for 5 min. Four millilitres of 1% sodium citrate were added and the solution was boiled gently for an additional 10 min while a deep orange-red colour developed. The pH of the gold was adjusted to the pH optimum of the mannanase activity (pH 4.5) by first determining the amount of HCl necessary to shift the pH in a small aliquot of colloidal gold, which was subsequently discarded. In order to avoid damaging the pH meter with flocculated gold, the aliquot was first stabilized against flocculation with the addition of 100 μl of 1% polyethyl glycol (PEG, 20,000 molecular weight), followed by measuring the amount of 1 N HCl that it took to adjust the pH. The calculated amount of HCl was then used to adjust the pH of 10 ml of unstabilized gold solution. A solution of purified mannanases or BSA (100 μl of 2 mg/ml protein) was added to the gold and stirred for 5 min to coat the gold particles with the protein. To check if the protein added was sufficient to stabilize the gold, an aliquot of protein-gold solution was mixed 1:1 with 10% sodium chloride. Unstabilized gold immediately turned blue, indicating flocculation, while stabilized enzyme-gold remained deep red following addition of the salt. After an additional 5 min of stirring, 500 μl of 1% PEG was added for additional stability. The enzyme-gold conjugate was centrifuged at 12,000 *g* for 1 h at 4°C to separate the probe from the unconjugated protein; the clear supernatant and dense black bottom pellet were discarded. The mobile red pellet was resuspended in 5 ml of 50 mM sodium citrate buffer and then the centrifugation was repeated. After resuspension in 2 ml of 50 mM sodium citrate, pH 4.5 with 0.1% PEG, the protein gold conjugate was stored at 4°C. The BSA/gold conjugate was washed and resuspended in 50 mM phosphate buffer, pH 7.0.

For labelling with antibody or enzyme/gold probes, gold and silver sections of samples embedded in LRGold resin (antibody) or LRWhite resin (mannanase) were picked up on formvar-coated nickel grids. Non-specific protein binding was blocked with 5% non-fat dried milk in 20 mM phosphate buffer, pH 7.0 containing 0.25 M sodium chloride and 0.1% Tween-20 (PBST). The excess milk was blotted off and the grids were transferred to a drop of antibody specific for anti-coniferin β-glucosidase diluted 1:10 with 1% milk in PBST buffer, and incubated for 1 h at room temperature. After washing with a spray of PBST for 20 s, the grids were incubated in a drop of buffer for 5 min and then incubated in protein A-10 nm gold diluted 1:75 with 1% non-fat dried milk in PBST for 1 h. Following washing with a spray and droplet incubation as above, the grids were washed with a spray of distilled water and post-stained. For mannanase/gold, following non-specific protein block, the milk was washed off with spray of phosphate buffer and the grids were transferred to a drop of citrate buffer at pH 4.5. Mannanase/gold probe was diluted 1:10 or 1:20 in 1% non-fat dried milk in PBST and the grids were floated on this solution at room temperature for 30 min. The samples were rinsed with a spray of citrate buffer for 20 s, followed by 5 min incubation in a drop of citrate buffer. Following a spray of distilled water; the grids were post-stained as above. As a control for non-specific protein binding, BSA-gold in phosphate buffer, pH 7.0, was substituted for mannanase-gold.

Results

Lignin histochemistry

Cryofixed differentiating secondary xylem of *Pinus contorta* var. *latifolia* displayed a developmental gradient from thin-walled cambial cells to mature xylem characterized by a lignified secondary wall and the absence of a living protoplast (Figs. 1 and 2). Light microscopy his-

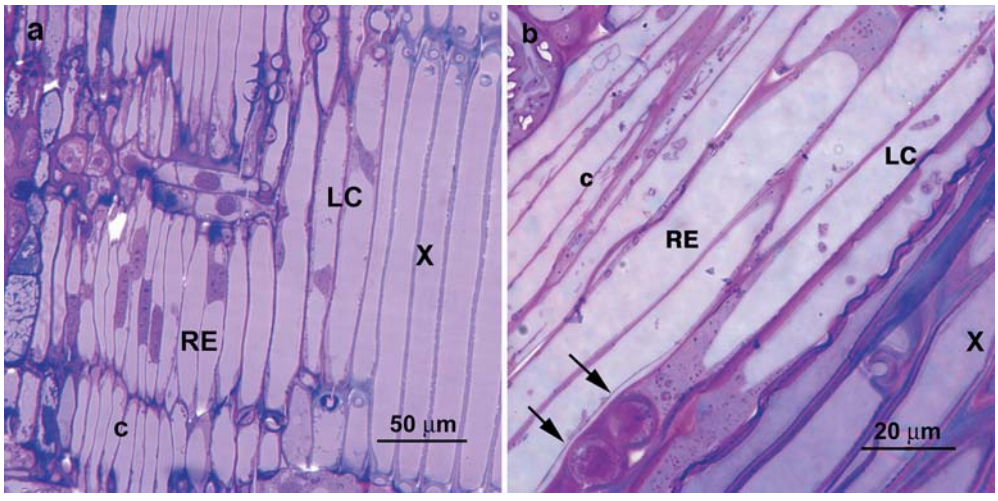

Fig. 1a, b. Light micrograph of longitudinal sections of inner bark of *Pinus contorta* showing intact morphology obtained with cryofixation. **a** Low magnification showing all cells from the phloem (*left*) to the mature secondary xylem (*right*). **b** Higher magnification of the zone of tracheid differentiation. Cambial zone cells have thin cell walls and prominent nuclei. Radially expanding cells exhibit the beginning of bordered pit formation (*arrow*) and secondary wall development. Lignifying cells (*LC*) have well-developed pits and the cell wall stained blue with toluidine blue, indicating the presence of lignin. Mature xylem lacks live protoplasts. (*c* Cambium, *RE* radially expanding cells, *LC* lignifying cells, *X* mature xylem)

tochemistry was used to determine the timing of the appearance of lignin in cryofixed samples, a key event in tracheid differentiation, and to pinpoint the timing of lignification relative to changes in cell structure and cell death. In the cryofixed samples observed using autofluorescence or toluidine blue staining, the first areas to display evidence of phenolic deposition were the middle lamellae, cell corners and bordered pits following S1 deposition, which is consistent with the results obtained by others using chemically fixed samples (Fig. 1). Full lignification of the tracheids was not complete until death of the protoplast was evident (Fig. 1a). Classical histochemical tests for lignin such as the Mäule (permanganate) and Weisner (phloroglucinol) stains also yielded results that were consistent with previous studies in which chemically fixed material was used (Srivastava 1966; Czaninski 1979). These stains were relatively insensitive, reacting only with the heavily lignified walls of mature tracheids whose protoplasts were dead, but not with the cell corners, middle lamellae or pits. Table 1 summarizes the timing of the appearance of cell wall polyphenolics in relation to the cambium, detected by the three techniques.

Ultrastructure of differentiating secondary xylem

When the ultrastructure of cryofixed pine cambium and developing xylem was examined using transmission electron microscopy, several structures were consistently observed: prominent oval nuclei, a large central vacuole with cortical cytoplasm, and plasma membranes that were tightly appressed to the cell wall (Fig. 2a–c). In cambial cells, mitotic chromosomes, phragmoplasts and newly deposited cell walls were often observed (data not shown; Rensing et al. 2002). Adjacent to the cambium in developing xylem, radial cell widths increased and the position of the nucleus changed from occupying the full width in the centre of the cell, to a position laterally displaced into the cortical cytoplasm (Figs. 1, 2c). At the end of the radial enlargement phase, secondary cell wall deposition began (Figs. 1, 2).

The change in cell wall nature from primary to secondary was accompanied by the appearance of prominent cortical microtubules that were aligned with the cellulose microfibrils (Fig. 2e, see also Figs. 3e, 4a). In both cambium and developing tracheids, prominent microfilament bundles were aligned parallel to the long axis of the cells (Fig. 2d). Golgi stacks were often close to these microfilament bundles (Fig. 2d), an observation consistent with the "stacks on tracks" model of Golgi movement (Boevink et al. 1998; Nebenführ et al. 1999). The appearance and distribution of both cytoskeletal elements correlated well with immunofluorescence studies of microfilament and microtubule distributions in developing secondary xylem (Abe et al. 1995; Funada et al. 1997; Chaffey and Barlow 2002).

Bordered pits began to develop late in the radial expansion phase (Figs. 1, 2b). The secondary wall deposition associated with pit formation was strongly correlated with the presence of abundant cortical microtubules as the wall thickened around the chamber containing the torus. The plasma membrane on the bottom of the chamber, adjacent to the torus, was often wavy and convoluted (Fig. 2f). This may represent an artefact of sample preparation in a delicate domain of the plasma membrane that could have been disturbed during dissection or pressurization.

With commencement of secondary cell wall formation in developing tracheids, a striking change occurred in Golgi morphology. When sections were stained for

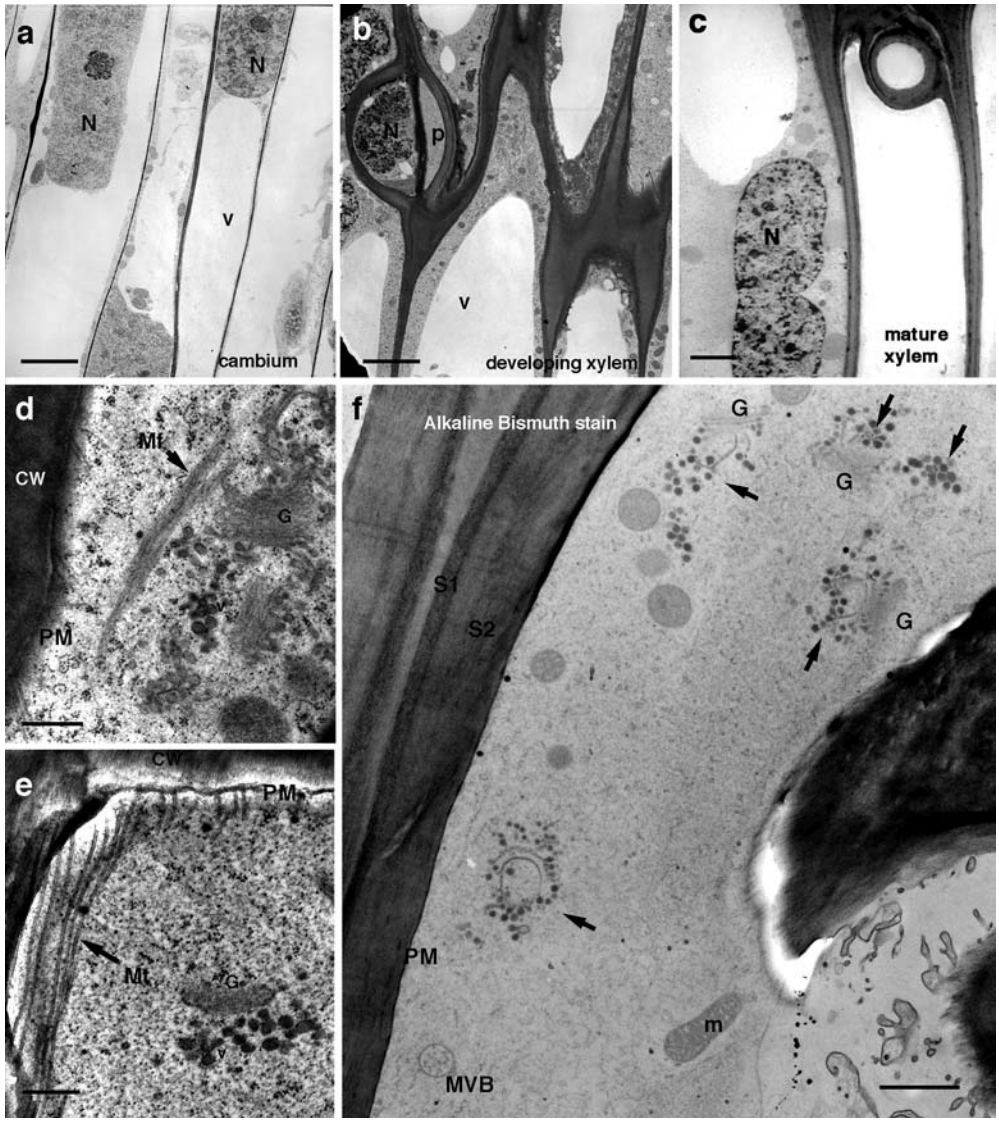

Fig. 2a–f. Longitudinal aspects of axial cambial and developing xylem cells prepared with high pressure freezing and transmission electron microscopy. **a** Cambial cells with prominent nuclei, large central vacuoles, and thin primary cell walls. **b** Developing xylem cells with bordered pit formation (plane of section slightly oblique) and nuclei laterally displaced into cortical cytoplasm. **c** Mature xylem cell adjacent to the last living protoplast with deformed nucleus and less dense cytoplasm. **d** Cortical cytoplasm of developing xylem cell with typical axial microfilament bundles, here associated with Golgi. **e** Tangential section through cortical cytoplasm of developing xylem cell with prominent cortical microtubules. **f** Tangential section through developing xylem cell following S1 and S2 secondary cell wall deposition stained with alkaline bismuth poststain for polysaccharides, emphasizing Golgi and post-Golgi vesicle clusters (*arrows*). *CW* Cell wall, *G* Golgi, *Mf* microfilament bundle, *Mt* microtubule, *m* mitochondrion, *MVB* multivesicular body, *p* pit, *PM* plasma membrane, *N* nucleus, *v* vacuole. *Bars*: **a–c** 5 μm, **d, e** 0.5 μm

Table 1. Appearance of lignin in cryofixed developing xylem of *Pinus contorta* var. *latifolia* as detected by three different histochemical techniques

	Technique		
	Autofluorescence	Mäule reagent (permanganate)	Wiesner reagent (phloroglucinol)
Mean number of cell layers between cambium and first reaction for lignin ± SD[a]	3.6 ± 0.2	4.8 ± 0.3	5.3 ± 0.4
First structures stained	Pits, cell corners, middle lamella	Wall proper	Wall proper

[a] $n = 10$ independent developing cambium samples for each technique

polysaccharides with alkaline bismuth (Park et al. 1987), the abundant Golgi vesicles were strongly labelled in tracheids producing secondary cell wall (Fig. 2f, arrows). Figure 3 compares the morphology of Golgi in cambial cells with that of Golgi in the developing xylem using conventional staining (Fig. 3a vs Fig. 3b–d). In cambium, Golgi had the typical structure of a cell secreting a primary cell wall, with a clear *cis*/*trans* polarity and variable amounts of small associated vesicles (Fig. 3a). In contrast, a few cell layers deeper in the developing xylem, Golgi were characterized by prominent, novel post-Golgi structures including branching *trans*-Golgi networks (TGN) and clusters of darkly staining vesicles associated with the TGN (Fig. 3b–d). Quantitatively, the appearance of grape-like clusters could be described as a significant increase in the

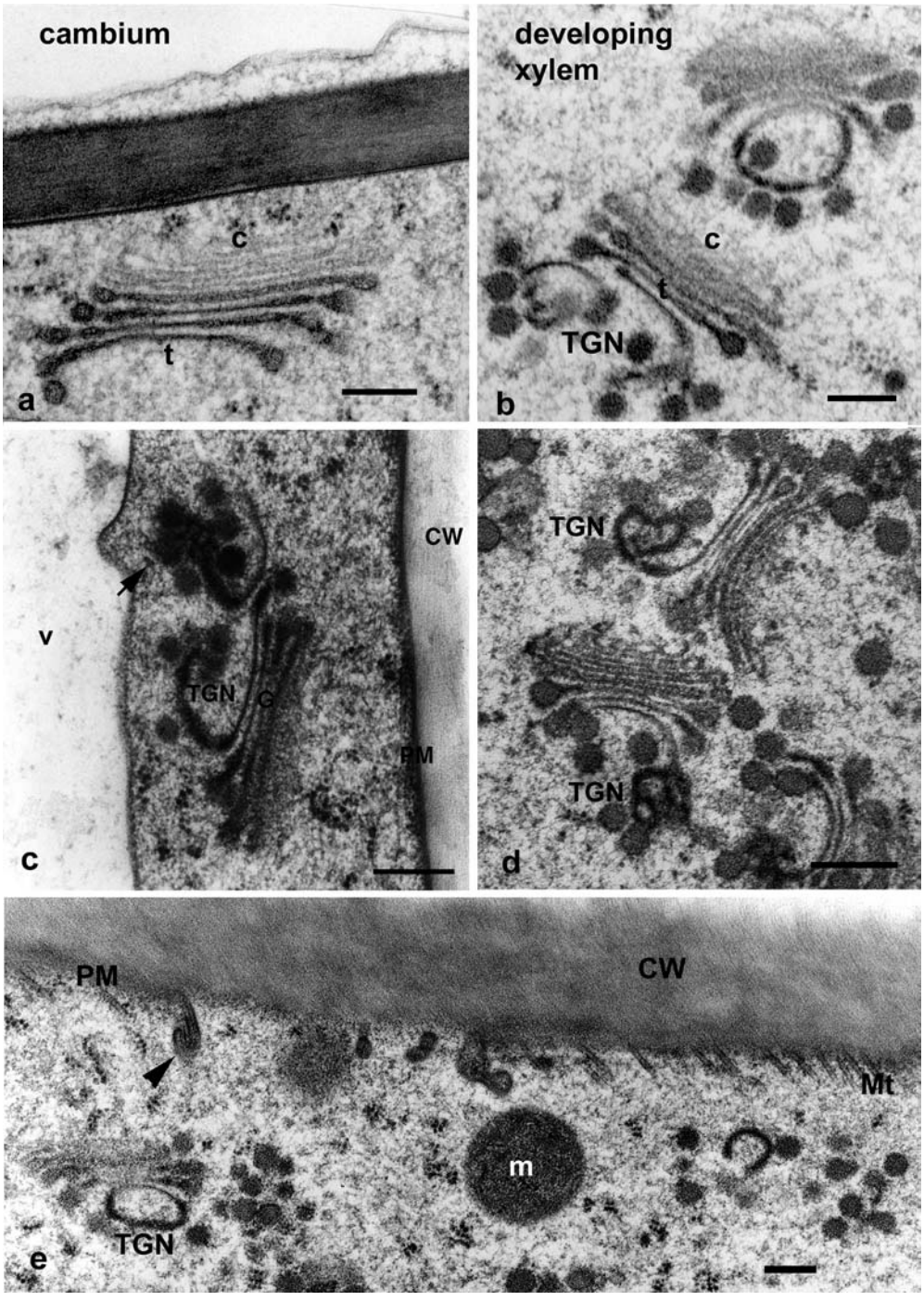

Fig. 3a–e. Golgi morphology in developing xylem cells. **a** Golgi from a cambial cell with typical "primary wall secreting" anatomy of strong *cis*/*trans* polarity in staining, small vesicles associated with stack, and small or indistinct TGN. **b–d** Golgi from developing xylem cells showing characteristic Golgi with elaborate, branching *trans*-Golgi networks and clusters of darkly staining vesicles. **e** Cortical cytoplasm in a developing tracheid with abundant cortical microtubules along the plasma membrane. An adjacent Golgi with a prominent *trans*-Golgi network and vesicles fusing with the plasma membrane (*arrow*). *c* cis cisterna of Golgi, *CW* cell wall, *Mt* microtubule, *m* mitochondria, *PM* plasma membrane, *t trans* cisterna of Golgi, *TGN trans*-Golgi network. *Bars* 0.25 μm

number of vesicles associated with the TGN in the developing xylem when compared to cambial cells (Table 2). The number of vesicles associated with the stack proper, or the number of cisternae per stack, were not significantly different in the cambium compared to developing xylem samples.

Serial section analysis showed that clusters of vesicles were both associated with a Golgi stack via the TGN as well as apparently free in the cytoplasm (as illustrated in Fig. 3c, arrow). The frequent appearance of vesicle clusters apart from, but adjacent to, Golgi stacks suggests that vesicle clusters were released from the Golgi stack as a set.

In the cortical cytoplasm of developing xylem cells, vesicles could be observed fusing with the plasma membrane (Fig. 3e). The membrane profiles of the fusing vesicles were collapsed, forming slit-like or horseshoe shaped structures. Similar observations were reported in cryofixed, freeze-fractured sycamore suspension cultured cells by Craig and Staehelin (1988), who interpreted the slits and horseshoes as fused secretory vesicles collapsing under turgor pressure. The similar density of the lumenal

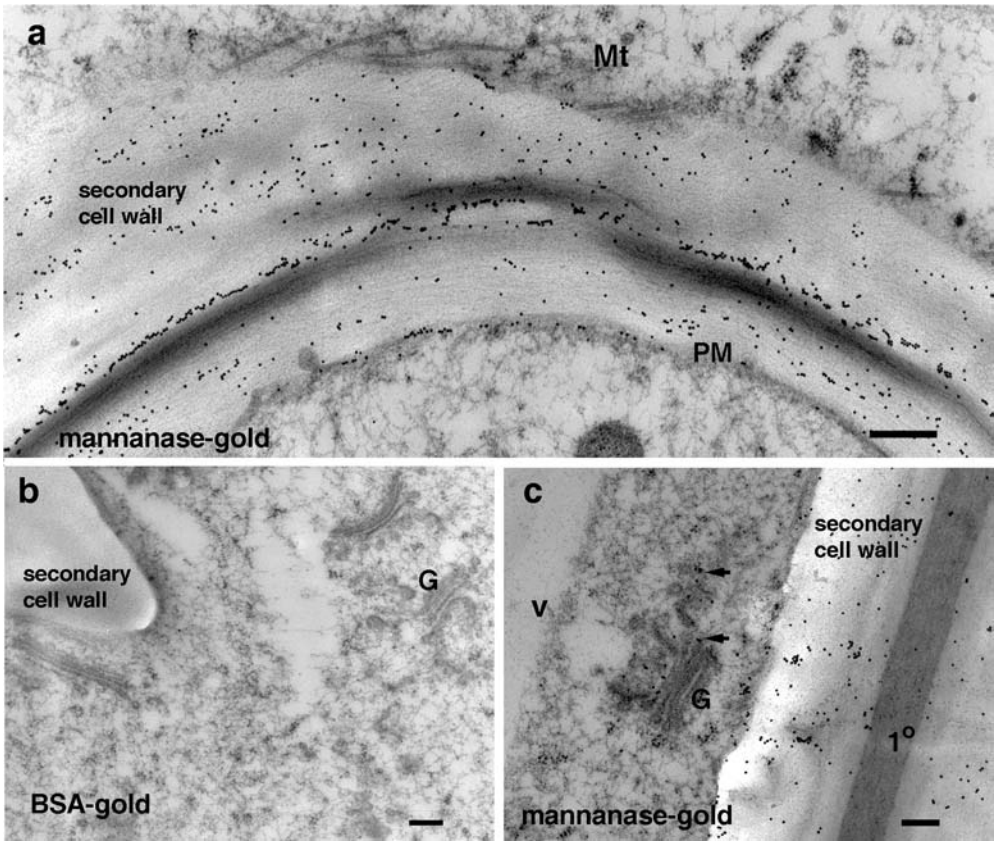

Fig. 4a–c. Mannanase-gold probe localization of mannans in developing xylem. *a* Developing pit with abundant cortical microtubules (*MT*) along the plasma membrane (*PM*) has mannanase-gold probe bound throughout secondary, but not primary cell wall. **b** Bovine serum albumin-gold probe (*BSA-gold*) did not bind strongly to developing pine tracheids. c Mannanase-gold probe bound to *trans*-Golgi network and adjacent vesicle clusters (*arrow*) as well as secondary, but not primary, cell wall layers. *G* Golgi, *1°* primary cell wall. *Bars* 0.25 μm

Table 2. Comparison of Golgi and associated vesicles in cambium or differentiating xylem cells during secondary wall development and early lignification. Mean ± SE; *TGN trans*-Golgi network)

Tissue	N	No. of cisternae/ stack	No. of vesicles/ TGN*	No. of vesicles/ stack
Cambium	21	5.2 ± 0.2	2.1 ± 0.8	2.5 ± 0.5
Developing xylem	31	5.7 ± 0.2	8.4 ± 0.7	1.8 ± 0.2

*Significantly different using paired *t*-test. Probability that means are equal = 0.0002

contents in the post-Golgi vesicles and fusing membrane profiles in this study strengthens this interpretation.

The developmental stage at which the novel Golgi and post-Golgi vesicle clusters became prominent in the developing pine secondary xylem correlated with secondary wall deposition as evidenced by abundant cortical microtubules and deposition of the S1 and S2 layers of the secondary cell wall (Figs. 2f, 3e). Temporally, this Golgi differentiation occurs just prior to the earliest lignification events in the cell corners and middle lamella. The Golgi then retained this characteristic morphology throughout xylem development until the death of the protoplast.

The final developmental event in xylogenesis is programmed cell death. The last living protoplast in the developing *Pinus* xylem typically contained a misshapen nucleus, with abundant scattered heterochromatin and an absence of nucleoli (Fig. 2c). The cytoplasm became less densely staining, with scattered ribosomes and dilated endothelial reticulum (ER), although the darkly staining Golgi with the characteristic morphology described above persisted. The tonoplast pulled away from the tight cortical position it occupied earlier and finally ruptures were clearly evident.

Cell wall polysaccharide biosynthesis

The appearance of the novel Golgi and Golgi-associated vesicle structures correlated with secondary wall biosynthesis. To more specifically study the secretion of the predominant hemicellulose, galactoglucomannan, in the *Pinus* secondary cell wall (Puls and Schuseil 1993), an enzyme-gold probe was designed to detect mannans based on enzyme-substrate specificity. Mannanase was purified from a commercial preparation of cell wall digesting enzymes and conjugated directly to colloidal gold. When applied to cryofixed freeze-substituted samples, the mannanase-gold probe bound strongly to the secondary cell wall of developing tracheids, as expected (Fig. 4a). Control probes made with BSA-gold did not significantly label the sections (Fig. 4b). Following radial expansion of the developing xylem, when the first secondary wall thickening was detected, the Golgi stacks, Golgi vesicles and the cell wall adjacent to

the plasma membrane in developing tracheids were clearly labelled with the mannanase probe (Fig. 4c). The *trans*-most cisterna of the Golgi stack was labelled more strongly than either the medial or *cis* cisternae. The mannanase-gold probe did not bind to the branching tubular domains of the TGN but the vesicle clusters associated with the TGN were labelled (Fig. 4c). Quantification of mannanase binding showed that the highest number of gold particles/μm^2 were located on the secondary cell wall and in the Golgi of the developing xylem cells, while the primary cell wall bound the probe only weakly (Fig. 5).

Coniferin-glucosidase localizes to the cell wall

The distribution of coniferin β-glucosidase was examined using a polyclonal antibody generated against purified recombinant *P. contorta* coniferin specific β-glucosidase expressed in *Escherichia coli* (Dharmawardhana et al. 1999). Due to the high phenolic levels in *Pinus* species, which resulted in bright autofluorescence, the primary antibody was detected with secondary antibody conjugated to colloidal gold, followed by silver enhancement for light microscopy (Fig. 6a). Labelling with colloidal gold was restricted to the cell walls of developing xylem, coinciding with secondary cell wall synthesis, suggesting that coniferin β-glucosidase epitopes are found exclusively in the walls of these cells. Replacement of the coniferin β-glucosidase antibody with pre-immune serum resulted in loss of secondary antibody labelling in developing xylem, indicating that the labelling obtained was specific for the glucosidase (Fig. 6b). Immunogold transmission electron microscopy confirmed these results, although in order to preserve antigenicity of the coniferin β-glucosidase epitopes, the developing xylem samples were prepared without osmium and embedded in LRGold resin, which was not optimal for morphology. Gold labelling was detected on the secondary cell wall of developing tracheids in the experimental antibody treatment but not in the preimmune control (Figs. 6d, e). In the developing tracheids where the secondary wall was labelled, no labelling of coniferin β-glucosidase epitopes could be detected in the cytoplasm and very little or no antibody binding was observed in the Golgi and associated vesicles (Fig. 6c). There was no binding of the anti-coniferin β-glucosidase to the primary cell wall of parenchymous ray cells in the cambium or secondary xylem (Fig. 6d, e).

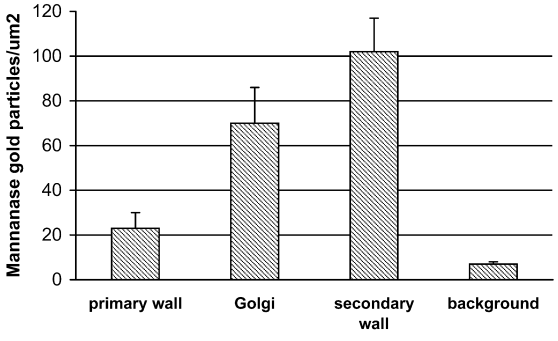

Fig. 5. Quantification of mannanase-gold binding on developing tracheids of *Pinus contorta*. Gold particles bound to the secondary cell wall and the Golgi in cells actively producing secondary cell walls, with some low binding to primary cell walls above background. Particles were counted by tracing the structure of interest, analysing the number of particles and measuring the area of the structure of interest to calculate particles per square micron. The selected area was then dragged into the background cytoplasm/vacuole and the number of gold particles within the randomly selected area counted to give the "background". Mean ± SD, 11 stem sections analysed from 3 experiments

Discussion

The biological question addressed in this study is: how are thin-walled cambial cells transformed into empty tracheids with strong, waterproof cell walls decorated with elaborate bordered pits? The structural changes that occur in the cytoplasm of tracheids within developing xylem give some indications of the cytoskeletal and endomembrane dynamics involved in achieving this developmental feat, which has been described as "the birth of a corpse" (McCann and Roberts 2000).

The cell structure of differentiating *P. contorta* secondary xylem undergoes dramatic changes in morphology from the cambium to the final stages of tracheid autolysis. The typical results of chemical fixation studies have shown the plasma membrane pulled away from the cell wall, abundant ballooning endomembrane structures that were interpreted as dilated ER being released into the cell wall space, or unusually large vesicles filled with fibrillar material that were continuous with the plasma membrane (Murmanis and Sachs 1969; Barnett 1977). By employing cryofixation, we see that the plasma membrane is instead smoothly pressed to the cell wall, both in the cambium and the developing xylem. The large central vacuole is intact until the final stages of programmed cell death, and the cytoplasm, which has not been exposed to the released contents of the vacuole, contains abundant organelles, notably Golgi and cytoskeletal elements. An earlier attempt to cryofix developing secondary xylem by plunge freezing (Inomata et al. 1992) also revealed changes in Golgi structure. However, the observations were limited because good cell preservation was obtained only in a thin peripheral layer where the surface of the specimen was rapidly cooled by the cryogen while the interior of the sample was destroyed by ice crystals. In our study, high pressure applied at the moment of freezing suppressed ice crystal formation, resulting in uniform freezing throughout the tissue. The suppression of ice crystals was probably aided by the high endogenous sucrose concentration in the developing xylem and cambium.

Our discovery of prominent Golgi and associated vesicles in the developing xylem cells indicates that Golgi-mediated secretion is important in xylem

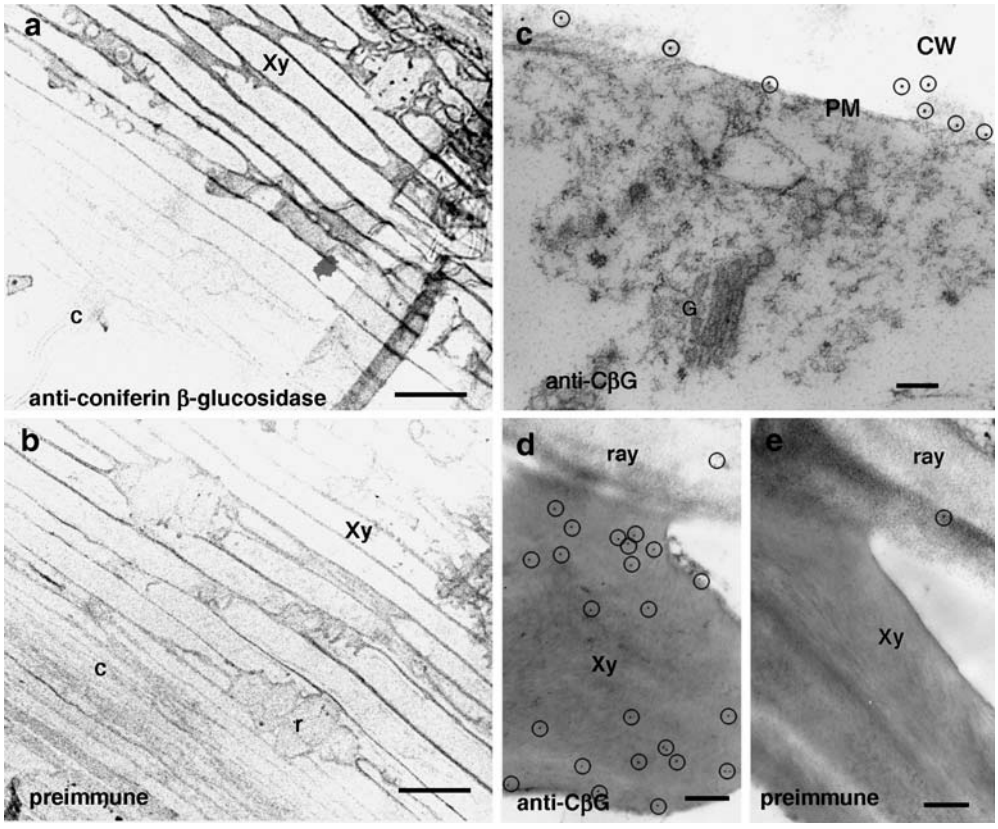

Fig. 6a–e. Subcellular localization of coniferin β-glucosidase in developing xylem. **a**, **b** Light microscopy of silver-enhanced immuno-gold binding. *a* Section reacted with polyclonal antibodies specific for coniferin β-glucosidase displays antibody binding in tracheid secondary cell walls. **b** Section reacted with preimmune serum shows diffuse background labelling. **c–e** Transmission electron microscopy of immunogold binding. **c** Thin section of a developing tracheid labelled with anti-coniferin β-glucosidase shows label in the apoplast but not in Golgi vesicles or cytoplasm. **d** Mature xylem tracheid adjacent to a parenchymous ray reacted with anti-coniferin β-glucosidase. Secondary cell wall of tracheid is labelled with anti-coniferin β-glucosidase while primary wall of the adjacent ray is not. **e** Mature xylem tracheid adjacent to a parenchymous ray reacted with preimmune serum. No labelling of secondary walls was evident. *α-CβG* Anti-coniferin beta-glucosidase, *c* cambium, *CW* cell wall, *PM* plasma membrane, *G* Golgi, *r* ray, *Xy* xylem. *Bars* **a, b** 5 μm, **c–e** 0.25 μm

development. The occurrence of vesicles as grape-like clusters associated with the TGN, adjacent to TGN, and remote from the Golgi in a clustered post-Golgi structure suggests that the vesicles mature as a group connected to each other by a membrane tubule. This pattern of membrane movement is consistent with a "cisternal maturation" model of the Golgi (Glick and Malhotra 1998), where each cluster could represent the maturation product of a single cisterna. Large post-Golgi structures have been observed in live mammalian cells secreting GFP-glycoprotein (Lippencott-Schwartz et al. 2000). It may be that these structures are susceptible to fragmentation upon exposure to glutaraldehyde treatment during chemical fixation, explaining why they have not been described in previous studies. The streaming of Golgi stacks in live plant cells (Boevink et al. 1998; Nebenführ et al. 1999) gives us a paradigm of dynamic Golgi traffic which is entirely compatible with the association of Golgi with microfilament bundles and shedding of vesicle clusters seen in the developing xylem in this study.

The central role of the Golgi in cell wall polysaccharide production is widely accepted and the results presented showing mannans in Golgi cisternae and vesicles during secondary wall biosynthesis are consistent with this role. An interesting consideration is whether the novel Golgi structures observed in association with secondary wall biosynthesis are secreting solely polysaccharides and proteins into the cell wall, or whether they may also deliver lignin precursors required for lignification of the secondary walls following polysaccharide deposition. The Golgi of the dividing cells of the cambium are also extremely active in cell wall matrix production associated with the new cell plate deposition, but the Golgi in the cambial cells lack the branching TGN and darkly staining clusters of vesicles found in developing tracheids. Because mannans were not localized to the branching TGN, it is possible that this structure is involved, not in polysaccharide secretion, but rather in the active phenylpropanoid metabolism of these cells undergoing incipient lignification.

The role of Golgi-mediated secretion in lignification is not well established, although secretion of monolignols or monolignol glucosides by vesicle fusion with the plasma membrane is often cited as one probable mech-

anism for precursor export (reviewed in Whetton and Sederoff 1995; Donaldson 2001). Autoradiographic studies have localized tritiated cinnamic acid to Golgi and associated vesicles in developing wheat coleoptile primary xylem (Pickett-Heaps 1968) and tritiated phenylalanine was localized to Golgi and associated vesicles in *Cryptomeria japonica* (Takabe et al. 1985). In the present study, dark staining Golgi vesicles were only found in osmicated samples and osmium has been used historically as a histochemical indicator of phenolics (Hayat 1981). During sporopollenin polyphenolic and polysaccharide deposition in *Ledebouria socialis* pollen, cryofixation revealed novel features including "post-Golgi structures" (Hess 1993) which were similar to those found here in developing xylem.

Further work is necessary to characterize the phenolic content of the prominent Golgi vesicles but our results are consistent with a role for Golgi-mediated secretion of phenolics. Co-secretion of monolignol glucosides and specific matrix polysaccharides (Terashima et al. 1995; Atalla 1998; Donaldson 2001) or dirigent proteins (Davin and Lewis 2000) could provide a mechanism for placing elements that control lignification in situ within the secondary wall of developing tracheids. The micro-environment in which dehydrogenative polymerization occurs has been postulated to be a guiding factor in producing the proper interunit linkages of native softwood lignin (Terashima et al. 1995, 1996; Davin and Lewis 2000). The demonstration that the presence of kraft pulp fragments can influence interunit linkage patterns (Guan et al. 1997; Sarkenen 1998) suggests that a relatively small amount of lignin deposited early during lignification could guide subsequent lignification events.

The early deposition of lignin in the middle lamellae and cell corners, while the cell is still actively secreting secondary cell wall, could be a mechanism to influence the polymerization of the large quantities of coniferin released from the dying cell. Leinhos and Savidge (1994) demonstrated that coniferin was found in high levels in protoplasts from *Pinus* and interpreted this as evidence for a vacuolar storage of coniferin. The immunolocalization of coniferin β-glucosidase in the secondary cell walls of developing tracheids suggests that lignin precursors are exported from these cells as glucosides rather than aglycones. According to this model, Golgi-mediated secretion of monolignols into the developing secondary cell walls would produce localized lignin polymerization. Release of coniferin-rich vacuolar contents upon cell death, in conjunction with wall localized coniferin β-glucosidase, would provide free coniferyl alcohol for polymerization into the bulk of the lignin matrix.

An alternative, or additional, mechanism of monolignol export, which our data do not exclude, is direct pumping of monolignols across the plasma membrane by membrane bound transporters. ABC transporters are a large gene family found in all organisms, where they transport lipids, toxins, and glutathione or glucose conjugates (Rea et al. 1998). There are many ABC transporters; 129 genes have been identified in the *Arabidopsis* genome and their functions are largely unknown (Sánchez-Fernández et al. 2001). In expressed sequence tag surveys of gene expression in developing secondary xylem of pine and poplar, ABC transporter genes are relatively abundant in maturing secondary xylem (Whetton et al. 2001; Hertzberg et al. 2001).

In summary, this study reveals novel features of developing secondary xylem in Pine, such as differentiating Golgi with prominent post-Golgi structures that have not been appreciated previously. A better understanding of the subcellular distribution of coniferin, and other phenylpropanoid lignin precursors, will be important to assessing what role these endomembrane systems play in the lignification process.

Acknowledgements This work was supported by the Natural Sciences and Engineering Research Council of Canada (NSERC) Strategic Grant to B.E.E. and C.J.D. and a NSERC University Faculty Award to A.L.S. The authors also acknowledge the infrastructure support of the Canadian Foundation for Innovation, BC Knowledge Development Fund and the Faculty of Science at UBC.

References

Abe H, Funada R, Imaizumi H, Ohtani J, Fukazawa K (1995) Dynamic changes in the arrangement of cortical microtubules in conifer tracheids during differentiation. Planta 197:418–421

Atalla RH (1998) Cellulose and hemicelluloses: patterns for the assembly of lignin. In: Lewis NG, Sarkenen S (eds) Lignin and lignan biosynthesis. American Chemical Society, Washington, DC, pp 172–179

Barnett JR (1977) Tracheid differentiation in *Pinus radiata*. Wood Sci Tech 11:83–92

Boevink P, Oparka K, Cruz SS, Hawes C (1998) Stacks on tracks: the plant Golgi apparatus traffics on an actin/ER network. Plant J 15:441–447

Chaffey N (1999) Cambium: old challenges-new opportunities. Trees 13:138–151

Chaffey N, Barlow P (2002) Myosin, microtubules, and microfilaments: co-operation between cytoskeletal components during cambial cell division and secondary vascular differentiation in trees. Planta 214:526–536

Craig S, Staehelin LA (1988) High pressure freezing of intact plant tissues. Evaluation and characterization of novel features of the endoplasmic reticulum and associated membrane systems. Eur J Cell Biol 46:80–93

Cronshaw J, Wardrop AB (1964) The organisation of cytoplasm in differentiating xylem. Aust J Bot 12:15–23

Czaninski Y (1979) Cytochimie ultrastructurale des parois du xyléme secondaire. Biol Cell 35:97–102

Davin LB, Lewis NG (2000) Dirigent proteins and dirigent sites explain the mystery of specificity of radical precursor coupling in lignan and lignin biosynthesis. Phytochemistry 123:453–461

Dharmawardhana DP, Ellis BE, Carlson JE (1995) A β-glucoside from Lodgepole Pine specific for the lignin precursor coniferin. Plant Physiol 107:331–339

Dharmawardhana DP, Ellis BE, Carlson JE (1999) cDNA cloning and heterologous expression of coniferin β-glucoside. Plant Mol Biol 40:365–372

Donaldson LA (2001) Lignification and lignin topochemistry-an ultrastructural view. Phytochemistry 57:839–873

Esau K (1965) Plant anatomy. Wiley, New York

Freudenberg K, Harkin JM (1963) The glucosides of cambial sap of spruce. Phytochemistry 2:189–193

Funada R, Abe H, Furusawa O, Imaizumi H, Fukazawa K, Ohtani J (1997) The orientation and localisation of cortical microtubules in differentiating conifer tracheids during cell expansion. Plant Cell Physiol 38:210–212

Glick BS, Malhotra V (1998) The curious status of the Golgi apparatus. Cell 95:883–889

Guan S-Y, Mlynar J, Sarkenen S (1997) Dehydrogenative polymerisation of coniferyl alcohol on macromolecular lignin templates. Phytochemistry 45:911–918

Gübitz GM, Hayn M, Urbanz G, Steiner W (1996) Purification and properties of acidic β-mannanase from *Scherotium rolfsii*. J Biotechnol 45:165–172

Hayat MA (1981) Fixation for electron microscopy. Academic Press, New York

Hertzberg M, Aspeborg H, Schrader J, Andersson A, Erlandsson R, Blomqvist K, Bhalerao R, Uhlen M, Teeri TT, Lundeberg J, Sundberg B, Nilsson P, Sandberg G (2001) A transcriptional roadmap to wood formation. Proc Natl Acad Sci 98:14732–14737

Hess MW (1993) Cell-wall development in freeze-fixed pollen: intine formation of *Ledebouria socialis* (Hyacinthaceae). Protoplasma 189:139–149

Inomata F, Takabe K, Saiki H (1992) Cell wall formation of conifer tracheids as revealed by rapid freeze and substitution method. J Electron Microsc 41:369–374

Leinhos V, Savidge RA (1994) Investigation of coniferin compartmentation in developing xylem of conifers during lignification. Acta Hortic 381:97–102

Lippencott-Schwartz J, Roberts TH, Hirschberg K (2000) Secretory protein trafficking and organelle dynamics in living cells. Annu Rev Cell Dev Biol 16:557–589

McCann MC, Roberts K (2000) Tracheary element formation: building up to a dead end. Trends Plant Sci 2:333–338

Murmanis L, Sachs IB (1969) Seasonal development of secondary xylem in *Pinus strobus* L. Wood Sci Technol 3:177–193

Nebenführ A, Gallagher LA, Dunahay TG, Frohlick JA, Mazurkiewicz AM, Meehl JB, Staehelin LA (1999) Stop-and-go movements of plant Golgi stacks are mediated by the actomyosin system. Plant Physiol 121:1127–1141

Park P, Ohno T, Kato-Kikuchi H, Miki H (1987) Alkaline bismuth stain as a tracer for Golgi vesicles of plant cells. Stain Technol 62:253–256

Pickett-Heaps JD (1968) Xylem wall deposition: radioautographic investigations using lignin precursors. Protoplasma 65:181–205

Puls J, Schuseil J (1993) Chemistry of hemicelluloses: relationship between hemicellulose structure and the enzymes required for hydrolysis. In: Coughlin MP, Hazlewood GP (eds) Hemicellulose and hemicellulases. Portland Press, London

Rea PA, Li Z-S, Lu Y-P, Drozdowicz YM, Martinoia E (1998) From vacuolar GS-X pumps to multispecific ABC transporters. Annu Rev Plant Physiol Plant Mol Biol 49:727–760

Rensing KH (2002) Chemical and cryo-fixation for transmission electron microscopy of gymnosperm cambial cells. In: Chaffey NJ (ed) Wood formation in trees: cell and molecular biology techniques. Taylor and Francis, New York, pp 65–81

Rensing KH, Samuels AL, Savidge RA (2002) Ultrastructure of vascular cambial cell cytokinesis in Pine seedlings preserved by cryofixation and substitution. Protoplasma (in press)

Samuels AL, Giddings TH, Staehelin LA (1995) Cytokinesis in tobacco BY-2 and root tip cells: a new model of cell plate formation in higher plants. J Cell Biol 130:1345–1357

Sánchez-Fernández R, Emyr-Davies TG, Coleman JOD, Rea PA (2001) The *Arabidopsis thaliana* ABC protein superfamily, a complete inventory. J Biol Chem 276:30231–30244

Sarkenen S (1998) Template polymerization in lignin biosynthesis. In: Lewis NL, Sarkenen S (eds) Lignin and lignan biosynthesis. American Chemical Society Symposium Series 697, Washington, DC, pp 194–208

Savidge RA (1989) Coniferin: a biochemical indicator of commitment to tracheid differentiation in conifers. Can J Bot 67:2663–2668

Savidge RA (1996) Xylogenesis. Int Assoc Wood Anat J 17:269–310

Shinji E, Shinji Y, Mizuhira V (1976) Histochemical study of a dermatophyte under an electron microscope: *Trichophyton mentagrophytes* cell wall. Acta Histochem Cytochem 9:292–305

Srivastava LM (1966) Histochemical studies on lignin. Tappi 49:173–183

Srivastava LM, O'Brien TP (1966) On the ultrastructure of cambium and its derivatives. I. Cambium of *Pinus strobus* L. Protoplasma 61:257–276

Takabe K, Fujita M, Harada H, Saiki H (1985) Autoradiographic investigation of lignification in the cell walls of Cryptomeria (*Cryptomeria japonica* D. Don). Mokuzai Gakkaishi 31:613–619

Terashima N, Atalla R, Ralph SA, Landucci LL, Lapierre C, Monties B (1995) New preparations of lignin polymer models under conditions that approximate cell wall lignification. I. Synthesis of novel polymer models and their structural characterisation by 13C-NMR. Holzforschung 49:521–527

Terashima N, Atalla R, Ralph SA, Landucci LL, Lapierre C, Monties B (1996) New preparations of lignin polymer models under conditions that approximate cell wall lignification. II. Structural characterisation of the models by thioacidolysis. Holzforschung 50:9–14

Terashima N, Nakashima J, Takabe K (1998) Proposed structure for protolignin in plant cell walls. In: Lewis NL, Sarkenen S (eds) Lignin and lignan biosynthesis. American Chemical Society Symposium Series 697, Washington, DC, pp 180–193

Terazawa M, Likuyama H, Miyake M (1984) Phenolic compounds in living tissue of woods. I. Phenolic β-glucosides of 4-hydroxycinnamyl alcohol derivatives in the cambial sap of wood. Mokuzai Gakkaishi 30:322–326

Whetton R, Sederoff R (1995) Lignin biosynthesis. Plant Cell 7:1001–1013

Whetton R, Sun Y-H, Zhang Y, Sederoff R (2001) Functional genomics and cell wall biosynthesis in loblolly pine. Plant Mol Biol 47:275–291

Wood TM, Bhat KM (1988) Methods for measuring cellulase activities. Methods Enzymol 160:87–102